ISSN 0021-3640, JETP Letters, 2017, Vol. 106, No. 8, pp. 498–502. © Pleiades Publishing, Inc., 2017.

CONDENSED MATTER

Neutron Investigations of the Magnetic Properties of $Fe_xMn_{1-x}S$ under Pressure up to 4.2 GPa[1]

G. Abramova[a, *], M. Boehm[b], J. Schefer[c], A. Piovano[b], G. Zeer[d], S. Zharkov[a, d], Y. Mita[e], and V. Sokolov[f]

[a] *Kirensky Institute of Physics, Federal Research Center KSC, Siberian Branch, Russian Academy of Sciences, Krasnoyarsk, 660036 Russia*

[b] *Institute Max von Laue–Paul Langevin, Grenoble, FR-38042 France*

[c] *Paul Scherrer Institut, Laboratory for Neutron Scattering and Imaging (LNS), Villigen PSI, CH-5232 Switzerland*

[d] *Siberian Federal University, Krasnoyarsk, 660041 Russia*

[e] *Materials Physics, Engineering Science, Osaka University Toyonaka, Osaka, 560-8531 Japan*

[f] *Institute of Inorganic Chemistry, Siberian Branch, Russian Academy of Sciences, Novosibirsk, 630090 Russia*

**e-mail: agm@iph.krasm.ru*

Received August 14, 2017; in final form, September 6, 2017

$Fe_xMn_{1-x}S$ belongs to the group of strong electron correlations compounds MnO. We present here experimental results for the antiferromagnetic iron–manganese sulfide system, based on X-ray and neutron diffraction studies. The neutron diffraction investigations were carried out at ambient conditions and at hydrostatic pressures up to 4.2 GPa in the temperature range from 65 to 300 K. Our results indicate that the Néel temperature of α-MnS increases up to room temperature by applying chemical (x_{Fe}) or weak hydrostatic pressure P. In $Fe_{0.27}Mn_{0.73}S$, the Néel temperature increases from 205(2) K (P = 0 GPa) to 280(2) K (P = 4.2 GPa) and the magnetization at 100 K decreases by a factor of 2.5 when the hydrostatic pressure increases from 0 to 4.2 GPa.

DOI: 10.1134/S0021364017200012

1. INTRODUCTION

High-pressure-induced phase transitions followed by the collapse of the localized magnetic moment are theoretically predicted [1, 2] and observed [3, 4] in strong electron correlations systems. α-MnS belongs to the transition-metal monoxides (MnO, FeO, CoO, and NiO) with rock salt crystal structure and antiferromagnetic structure of type II [5–7]. The Mott transition in MnS at room temperature has been revealed recently by the spectroscopic data at high pressure (P_c = 26 GPa) [7]. A rocksalt-to-MnP phase transition under compression accompanied by the $Mn^{2+}(d^5)$ spin-state transition from $S = 5/2$ to $S = 1/2$ was found by Wang et al. [7] using pressure-dependent X-ray emission spectroscopy. As the radius of the $3d$-Fe^{2+} ion (0.83 Å) is lower than the Mn^{2+} one (0.92 Å), we expect that chemical pressure induced by the substitution of Mn by Fe will change the physical properties of MnS, similar to external pressure P. Our previous investigations [8] indicate that the cation substitution of the manganese ions in $Me_xMn_{1-x}S$ leads to a decrease in the cubic cell parameter a: in the case of Fe from a = 5.224 Å ($x_{Fe} = 0$) to a = 5.17 Å ($x_{Fe} = 0.29$). This latter value of the cell parameter corresponds to the value observed in MnS with an external pressure of 4–5 GPa. Neutron diffraction experiments of $Fe_xMn_{1-x}S$ samples have been performed using the thermal powder diffractometer D1A@ILL and the single crystal diffractometer TriCS@SINQ. Results indicate an increase in the Néel temperature T_N from 150 K for $x = 0$ to ≈200–220 K for $x \approx 0.29$ [8]. The Mott transition in $Fe_xMn_{1-x}S$ was observed at room temperature. The samples with $0.25 < x < 0.3$ have semi-metal electrical properties and an optical reflection spectrum which is for $x = 0.25$ and room temperature almost independent of pressure [8, 9]. The increase in the cell parameter is accompanied by a decrease in the resistance by six orders of magnitude in comparison to MnS.

In this investigation, we present novel data of the semimetal $Fe_{0.27}Mn_{0.73}S$ compound under external pressure P using neutron powder diffraction technique.

[1] The article is published in the original.

2. SAMPLES AND EXPERIMENTAL TECHNIQUE

Microstructures and chemical compositions of $Fe_xMn_{1-x}S$ single crystals were investigated by scanning electron microscopy (SEM) using a JEOL JSM-7001F equipped with an energy dispersive X-ray spectrometer (Oxford Instruments). The Néel temperature has been determined for $Fe_xMn_{1-x}S$ single crystals and polycrystalline sample with $0.05 \le x \le 0.29$ at ambient pressure, using the D1A, IN3 (both ILL, Grenoble) and TriCS (SINQ/PSI, Villigen) neutron instruments. A neutron powder diffraction study of $Fe_xMn_{1-x}S$ ($x = 0.27$, ~30 mm^3 powder) has been carried out at the high flux spectrometer IN8 (Institut Laue–Langevin, ILL) using the elastic configuration ($k_i = k_f = 2.662$ Å^{-1}, $\lambda = 2.36$ Å) at temperatures between 2 and 300 K and pressure up to 42 kbar (4.2 GPa). To reject higher harmonics contamination, a PG filter has been installed after the sample. The polycrystalline sample was mixed with a pressure-transmitting medium (deuterated ethanol/methanol) and loaded to the Paris–Edinburgh cell. To control the temperature, we installed a calibrated Cernox, CX1050, X47001 thermoelement inside the cryostat. At ambient pressure, we measured of the neutron diffraction spectra in the temperature range of 2 and 250 K. Pressure (P) had to be applied at elevated temperature (77–290 K) to avoid freezing of the pressure transmitting medium. For fast cooling of the Paris–Edinburgh (PE) cell within the closed cycle cryostat having a limited cooling power, liquid N_2 was filled directly into the sample area and pumped out once a temperature of around $T = 80$ K has been reached. Due to the large mass of the PE cell, there was a large inertia. The whole system was too slow to wait for the stabilization of selected predefined temperatures. Alternatively, we have chosen fixed values for the external heating power in order to obtain heating rates adapted to our data collection times. The method and technique for neutron diffraction studies under pressure are described in [10, 11]. The compressor was used in pressure experiments. The sample pressure value at neutron investigations was determined from the ILL pressure calibration curves.

For higher pressures and room temperature, X-ray diffraction (XRD) powder measurements have been performed using a diamond anvil cell, and a 1 : 4 mixture of ethanol and methanol as a pressure-transmitting medium. These measurements were carried out at Osaka University. The pressure was determined by using the ruby fluorescence method.

3. EXPERIMENTAL RESULTS AND DISCUSSION

Figure 1 shows the change in the cubic cell volume (NaCl structure) determined from powder and single crystal neutron diffraction data for $Fe_xMn_{1-x}S$ under chemical pressure (X). Values range from an external pressure $P = 0$ to 6 GPa and at room temperature (RT). For comparison, the literature data for MnS [7] are added in Fig. 1. One easily can see that the lattice compression of MnS under chemical pressure (X) at ambient and fixed temperature is similar to its dependence on pressure (P). It has been found, that the lattice volume of MnS decreases by 2.6% under chemical pressure X(Fe) and by 2.9% under hydrostatic pressure for $x = 0.18$.

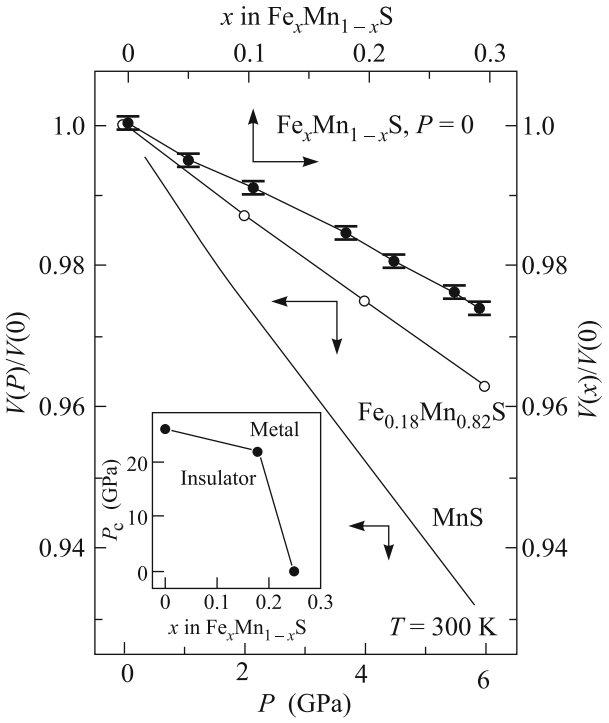

Fig. 1. Normalized cell volume V for $Fe_xMn_{1-x}S$ at RT versus the composition (x) and pressure (P): (top/right) $V(x)/V(x = 0)$ under ambient pressure $P = 0$ and (bottom/left) $V(P)/V(P = 0)$ under pressure for $x = 0.18$. The lattice parameters a (NaCl-structure type) were measured by X-ray diffraction for $x = 0$ (MnS) and neutron diffraction (D1A and IN8@ILL, TriCS@SINQ). For comparison, the literature value for MnS has been added [7, 17, 18]. Insert: the dependence of the critical pressure P_c for the transition from insulate to semimetal state in the system $Fe_xMn_{1-x}S$.

The investigations of the chemical compositions of $Fe_xMn_{1-x}S$ indicate that the real chemical composition for each sample differs from the indicated one by not more than of $\Delta x = \pm 0.02$.

Insert of Fig. 1 presents the dependence of the critical pressure P_c for the transition from insulate to semimetal state in the system $Fe_xMn_{1-x}S$, obtained from the data investigations of samples by the optical, structural and electrical methods [12–14]. The data

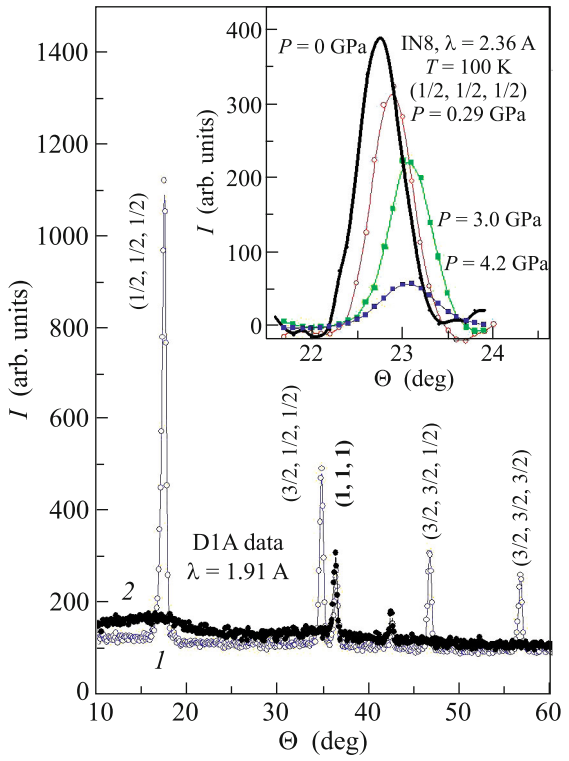

Fig. 2. (Color online) Neutron diffraction spectra of $Fe_{0.27}Mn_{0.73}S$ in the antiferromagnetic state at 100 K (marked *1*, open icons) and in the paramagnetic state (240 K, marked *2*, closed icons) are presented. The data have been collected on the thermal powder diffractometer D1A ($\lambda = 1.91$ Å) at ambient pressure. The insert shows the change in the magnetic peak (1/2, 1/2, 1/2) under hydrostatic pressure at 100 K. The data has been obtained at the high flux spectrometer IN8@ILL ($\lambda = 2.36$ Å).

indicate that the critical pressure P_c decreases with increasing chemical pressure (X) at room temperature.

Figure 2 shows the neutron diffraction spectra of polycrystalline $Fe_{0.27}Mn_{0.73}S$ samples measured at ambient conditions and at 100 K using D1A@ILL ($\lambda = 1.91$ Å) for the antiferromagnetic state (open icons, 1) and 240 K for paramagnet state (closed icons, 2). We followed the powder line for the magnetic (1/2, 1/2, 1/2) reflection for $Fe_{0.27}Mn_{0.73}S$ to establish the magnetic phase diagram under pressure. The insert of Fig. 2 presents these results at 100 K. To get reasonable statistics within the accepted temperature intervals available, the measuring time was adapted to the temperature inertia of the setup. Simple Gaussian function fitting was used for evaluating the magnetic peaks as a function of temperature. For the analysis of the data, the fitting parameters (background, the center of the peak, width FWHM and maximum intensity) were iteratively adjusted and fixed for the complete set of pressure values P. The intensities were normalized to a neutron monitor value of 15000 corresponding to a counting time of around 1 min per temperature. The square roots of the integrated intensities ($|F_{mag}|$) of the neutron peak (1/2, 1/2, 1/2) at 100 K are illustrated in Fig. 3 as a function of the corrected regulation temperature T_1, the temperature T_2, and the interpolated real temperature of the sample T_{inter}. The temperature dependence of the square root of the intensities ($|F_{mag}|$) at the individual pressure values is proportional to the magnetization of the magnetic sublattice

$$M \approx \sqrt{I}, \quad (1)$$

I is the integrated intensity of the magnetic peak.

The magnetization close to the critical transition temperature can be described by a power law with the critical exponent for the magnetization β:

$$M = M_0[(T_N - T)/T_N]^{\beta}. \quad (2)$$

Figure 3 shows the "magnetization" as obtained from Eq. (1) as a function of the interpolated temperatures. Lines are fits with the help of Eq. (2). The obtained parameter of β lies within the interval 0.42–0.5 and is intermediate between the Heisenberg 3D (0.367) and Ginzburg–Landau (0.5) models. The choice of the temperature range influences the fitting parameters.

We found a decrease in the sublattice magnetization ($|F_{mag}| \sim \sqrt{I}$, I is the peak intensity) with increasing hydrostatic pressure for $Fe_xMn_{1-x}S$ with $x = 0.27$ (Fig. 3). For example, at 100 K the magnetization $|F_{mag}|$ of the sample decreases nonlinearly by a factor of 2.5 with increasing pressure up to 42 kbar (4.2 GPa).

Figure 4 shows the (a) lattice parameter and (b) magnetization $|F_{mag}|$ under pressure at $T = 100$ K. The results are based on the observed change in the position (Θ), and the integrated intensity of the magnetic peak (1/2, 1/2, 1/2) at different pressure values. Figure 4 presents the relative values.

The Néel temperature of the $Fe_{0.27}Mn_{0.73}S$ sample at ambient pressure was derived from D1A and IN8 data, $T_N = 205 \pm 5$ K. The shift of the Néel temperature up to 280 K was detected with increasing pressure up to 42 kbar (4.2 GPa). Figure 5 presents the shift of the Néel temperature in $Fe_xMn_{1-x}S$ under ambient pressure due to the chemical lattice pressure (due to the cationic substitution, x) and the shift of the Néel temperature for the fixed composition ($x = 0.27$, $Fe_{0.27}Mn_{0.73}S$) under hydrostatic pressure (P).

The obtained results indicate that the Néel temperature of α-MnS increases up to room temperature by applying chemical or weak hydrostatic pressure. The mechanism of the increase in the Néel temperature can be associated with a NaCl-lattice compression and an increase in the exchange integral due to the increase in the degree of covalence and the metallization.

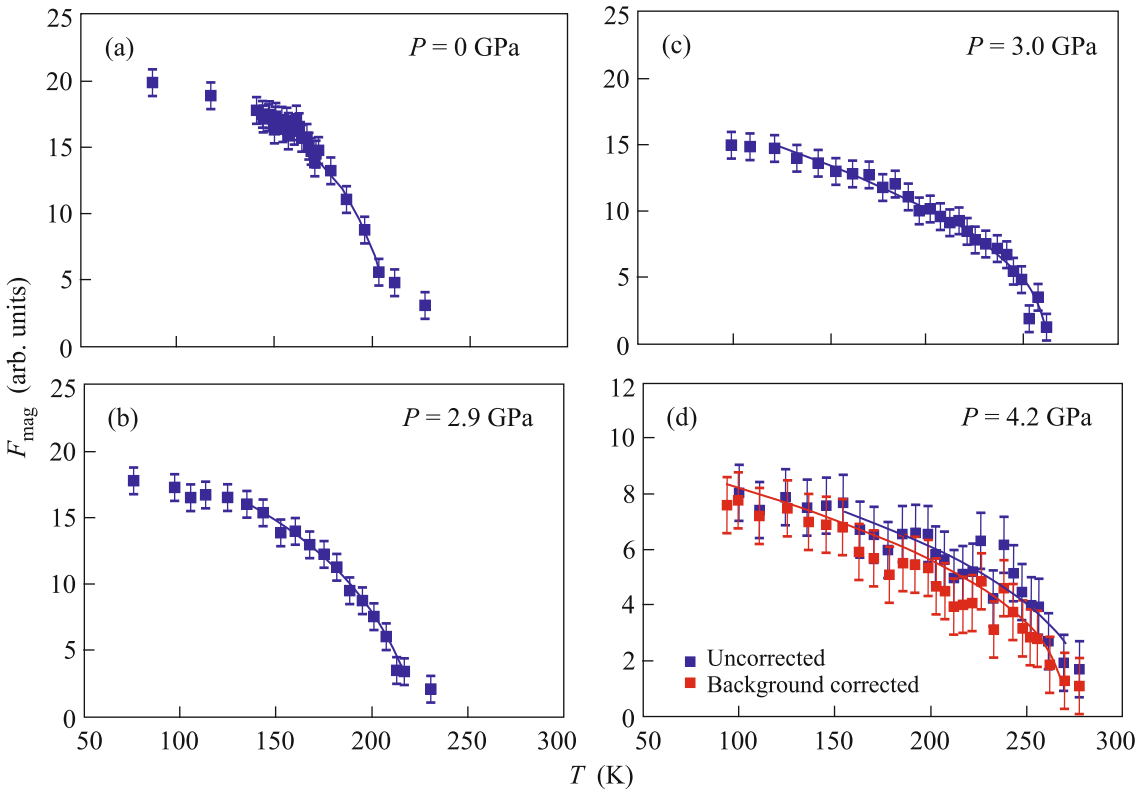

Fig. 3. (Color online) $|F_{mag}|$ for $Fe_{0.27}Mn_{0.73}S$ versus the interpolated temperature T_{inter} for different hydrostatic pressure values P (data: IN8@ILL).

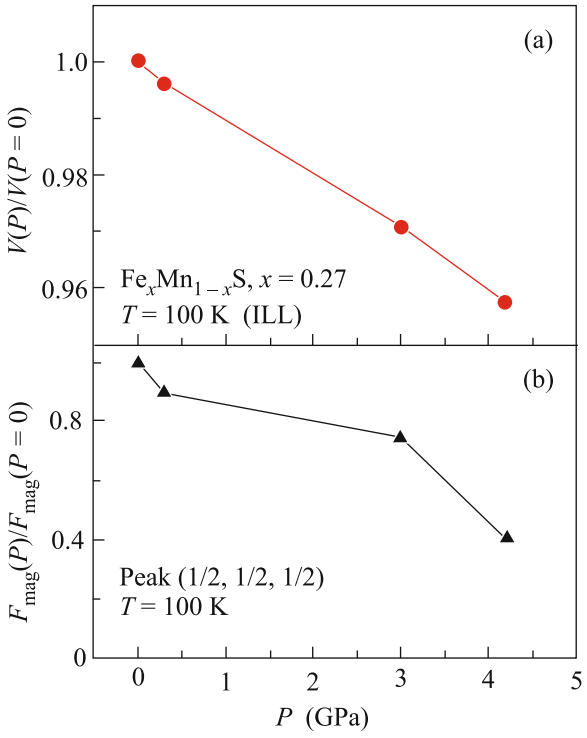

Fig. 4. (Color online) (a) Normalized lattice volume and (b) the magnetization F_{mag} for $Fe_{0.27}Mn_{0.73}S$ at $T = 100$ K versus the hydrostatic pressure.

To clarify the mechanism for the found decrease in the intensity of the magnetic peak, additional studies are needed, for example, the Mössbauer investigation of the samples at low temperatures. The local distortion of the octahedral coordination of the cubic lattice at 300 K in the $Fe_xMn_{1-x}S$ system for $0.15 < x < 0.29$ had previously been established by Mössbauer spectroscopy [15]. The increase in the octahedral coordination distortion with hydrostatic pressure may lead to a spin crossover and transition of the magnetic Fe^{2+} and Mn^{2+} ions from the high spin (HS) to the low-spin (LS) state due to the change in splitting of the d-levels for Fe^{2+} and Mn^{2+} ions by a crystalline field. For pure MnS ($S = 5/2$) this transition to an intermediate spin state with $S = 3/2$ (IS) is observed in the 15–30 GPa range [7]. The change in the magnetic state for pure α-MnS (unlike classic $BiFeO_3$ [2, 3]) occurs over a wide range of pressures. Low-spin state is observed at 26 GPa according to [7]. The electronic doping in a solid solution $Fe_xMn_{1-x}S$ causes a decrease in the value of the critical pressure P_c of the transition (insert of Fig. 1). From here, we can suppose that the critical hydrostatic pressure P_c for the semimetal sample $Fe_xMn_{1-x}S$ with $x = 0.27$ lower than MnS, and the observed decrease in the neutron intensity $|F_{mag}|$ may be the result of the change in the ion spin state.

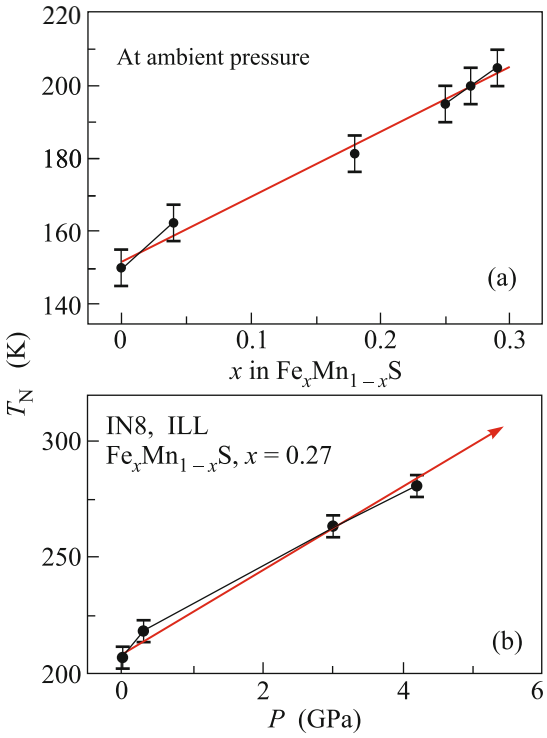

Fig. 5. (Color online) Dependence of the Néel temperature T_N on (a) chemical pressure due to doping for $Fe_xMn_{1-x}S$ at hydrostatic pressure $P = 0$ (b) for $Fe_{0.27}Mn_{0.73}S$ as a function of elevated hydrostatic pressure P. The data (a) has been obtained using the neutron powder diffractometer D1A@ILL and the single crystal neutron diffractometer TriCS@SINQ, whereas the data (b) has been obtained from the spectrometer IN8@ILLA shift of T_N has been observed, due to chemical pressure X at $P = 0$; ($dT_N/dX = 1.96$ K/at % Fe) and due to external pressure at 100 K ($dT_N/dP = 17.9$ K/GPa).

The magnetization decrease may also be due to the Villary piezomagnetic effect, which is characteristic of antiferromagnets and indicates a change in the magnetic lattice symmetry. Such an effect was observed for $Fe_{81}Si_{3.5}B_{13.5}C_2$ [15]. The inverse magnetostrictive effect was observed earlier for $Fe_xMn_{1-x}S$, $x = 0.27$ [16].

The further investigation and clarify the mechanisms of the pressure influence on the magnetic properties of $Fe_xMn_{1-x}S$ are actual.

4. CONCLUSIONS

The presented results of the neutron investigation showed that the structural and magnetic properties of the solid solutions of manganese monosulfide $Fe_xMn_{1-x}S$ were structurally dependent. These compounds are perspective for applications, e.g., as magnetoelastic sensors due to the low values of the pressure and for further research to understand the mechanisms of changing the magnetic properties under chemical and hydrostatic pressure.

We acknowledge the beam time used at D1A and IN8 of the Institut Laue–Langevin Grenoble (ILL) and the single instrument TriCS (replaced now by ZEBRA) at the Swiss Spallation Neutron Source SINQ/Paul Scherrer Institut, Villigen PSI.

REFERENCES

1. J. Kunes, A. V. Lukoyanov, V. I. Anisimov, R. T. Scalettar, and W. E. Pickett, Nat. Mater. **7**, 198 (2008).
2. R. E. Cohen, I. I. Mazin, and D. G. Isaak, Science **275**, 654 (1997).
3. I. S. Lyubutin, S. G. Ovchinnikov, A. G. Gavriliuk, and V. V. Struzhkin, Phys. Rev. B **79**, 085125 (2009).
4. I. S. Lyubutin and A. G. Gavriliuk, Phys. Usp. **52**, 989 (2009).
5. L. Corliss, N. Elliott, and J. Hastings, Phys. Rev. **104**, 924 (1956).
6. Y. Mita, Y. Ishida, M. Kobayashi, S. Endo, and S. Mochizuki, Physica B **359–361**, 1192 (2005).
7. Y. Wang, L. Bai, T. Wen, L. Yang, H. Gou, Y. Xiao, P. Chow, M. Pravica, W. Yang, and Y. Zhao, Angew. Chem. Int. Ed. **55**, 1 (2016).
8. G. Abramova, J. Schefer, N. Aliouane, M. Boehm, G. Petrakovskiy, A. Vorotynov, M. Gorev, A. Bovina, and V. Sokolov, J. Alloys Compd. **632**, 563 (2015).
9. G. M. Abramova, N. V. Volkov, G. A. Petrakovskiy, Y. Mita, O. A. Bayukov, D. A. Velikanov, A. M. Vorotynov, V. V. Sokolov, and A. F. Bovina, JETP Lett. **86**, 371 (2007).
10. S. Klotz, J.-C. Chervin, P. Munsch, and G. le Marchand, J. Phys. D: Appl. Phys. **42**, 075413 (2009).
11. S. Klotz, *Techniques in High Pressure Neutron Scattering* (CRC, Taylor and Francis, Boca Raton, FL, 2013).
12. Y. Ishida, Y. Mita, M. Kobayashi, S. Endo, and S. Mochizuki, J. Magn. Magn. Magn. **272–276**, 428 (2004).
13. G. Abramova, N. Volkov, G. Petrakovskiy, V. Sokolov, M. Boehm, O. Baukov, A. M. Vorotynov, A. Bovina, and A. Pischjugin, J. Magn. Magn. Mater. **320**, 3261 (2008).
14. Y. Mita, T. Kagayama, G. M. Abramova, G. A. Petrakovskii, and V. V. Sokolov, J. Korean Phys. Soc. **63**, 325 (2013).
15. G. M. Abramova, G. A. Petrakovskiy, O. A. Bayukov, V. A. Varnek, V. V. Sokolov, and A. F. Bovina, Phys. Solid State **50**, 237 (2008).
16. B. Kundys, Yu. Bukhantsev, H. Szymczak, M. R. J. Gibbs, and R. Zurek, J. Phys. D: Appl. Phys. **35**, 1095 (2002).
17. G. M. Abramova, G. Petrakovskiy, R. Zuberek, A. Nabialek, M. Boehm, V. Sokolov, and A. F. Bovina, JETP Lett. **90**, 207 (2009).
18. C. A. McCammon, Phys. Chem. Miner. **17**, 636 (1991).